New Measurement of ^{165}Ho Neutron Capture Cross Section Data*

Su-Ya-La-Tu Zhang,[1,2,†] Yong-Shun Huang,[1,2] Wei Jiang,[3,4] Jie Ren,[5] Rui-Rui Fan,[3,4]
De-Xin Wang,[1,2] Chun-Lei Zhang,[6] Guo-Li,[1,2] Dan-Dan Niu,[1,2] and Mei-Rong Huang[1,2]

[1]*Institute of Nuclear Physics, College of Physics and Electronic Information, Inner Mongolia Minzu University, Tongliao 028000, Inner Mongolia, China.*
[2]*Inner Mongolia Joint Key Laboratory for Nuclear and Radiation Detection, Tongliao 028000, Inner Mongolia, China.*
[3]*Institute of High Energy Physics, Chinese Academy of Sciences, Beijing 100049, China.*
[4]*Spallation Neutron Source Science Center, Dongguan 523803, China*
[5]*China Institute of Atomic Energy, Beijing 102413, China.*
[6]*College of Nuclear Science and Technology, Beijing Normal University.*

The neutron capture cross section data for ^{165}Ho were measured at the back streaming white neutron beam line (Back-n) of the China Spallation Neutron Source (CSNS) using total energy detection systems, which is comprise a set four C_6D_6 scintillator detectors coupled with pulse height weighting techniques. The resonance parameters were extracted using the multi-level multichannel R-matrix code SAMMY, fitting the measured capture yields of the ^{165}Ho(n,γ) reaction in the neutron energy range below 100 eV. Subsequently, the resonance region capture cross sections were reconstructed on the basis of the obtained parameters. Furthermore, the unresolved resonance average cross section of ^{165}Ho(n,γ) reaction was determined relative to the standard sample ^{197}Au within the neutron energy range of 2 keV to 1 MeV. The experimental data were compared with the recommended nuclear data from the ENDF/B-VIII.0 library, as well as the calculations of the TALYS-1.9 code. The comparison indicates that the measured ^{165}Ho(n,γ) cross sections agree well with these data. The present results are significant for the evaluation of the ^{165}Ho neutron capture cross section data, enhancing the quality of the evaluated nuclear data libraries, and providing valuable guidance for nuclear theoretical models and nuclear astrophysical studies.

Keywords: Holmium, neutron capture reaction, cross section data, total energy detection principle, C_6D_6 scintillator detector, China Spallation Neutron Source.

I. INTRODUCTION

Nuclear data is used to describe the physical properties of atomic nuclei and their interactions. Neutron data plays a key role in fundamental nuclear physics research and in the development of nuclear energy and nuclear technology [1, 2]. Neutron capture cross-sectional data are extremely important for stellar nucleosynthesis of heavy elements, medical applications, radiation dosimetry, transmutation of nuclear waste and advanced nuclear energy system [3–5].

Many laboratories worldwide, including CERN n_TOF [6], Los Alamos National Laboratory DANCE [7], Karlsruhe [8], and GELINA [9] have developed two types of detection systems for the online measurement of neutron capture cross sections. These systems include the gamma-ray total energy and total absorption detectors. The total energy detection systems generally use a low efficient C_6D_6 scintillator detector, which is suitable for stable nuclide measurement of high cross-section and large samples. The total absorption detection systems often use BaF_2 crystal detector array with high energy resolution, good time resolution, low neutron sensitivity and high efficiency to carry out neutron capture measurement for small size sample, low cross section and unstable radionuclides. The China Spallation Neutron Source (CSNS) [10] provide neutrons via high intensity 1.6 GeV proton beam bombarding on a tungsten target. The back streaming neutron beam line (Back-n) is positioned in reverse direction of proton beam at the CSNS with a flight pass length of approximately 80 meters. Figure 1 shows the schematic view of the experimental setup of the CSNS Back-n. Currently, five types of spectrometers have been constructed at the Back-n facility for the purpose of nuclear data measurement. These instruments include a set of four C_6D_6 detectors [11–13] and a 4π BaF_2 detector array, referred to as the Gamma Total Absorption Facility II (GTAF-II) [14], which are utilized for neutron capture measurements. Additionally, a multilayer fast ionization chamber (FIXM) is employed for fission reaction measurements [15], while a neutron total cross section detector (NTOX) is specifically designed for total cross section assessments [16]. Furthermore, light-charged particle detectors (LPDA) are utilized for measuring light charged particle emissions [17].A detailed description of the spectrometers can be found in Refs [18].

Holmium (Ho), comprised entirely of the isotope ^{165}Ho with 100% natural abundance, has been proposed as a standard for neutron capture cross section measurements. This is attributed to its favorable radioactive half-life and the substantial capture cross-section observed at the first resonance peak, which is essential for "saturation resonance" calibration [19–21]. Only a few experimental studies have been performed in the past for the low energy resonance region, and large discrepancies are observed between the reported

* This work was supported by the National Natural Science Foundation of China (No.12465024,12365018,U2032146); Inner Mongolia National Science Foundation (No.2024ZD23,2024FX30,2023MS01005); Program for Innovative Research Team in Universities of Inner Mongolia Autonomous Region (NMGIRT2217); Program for Young Talents of Science and Technology in Universities of Inner Mongolia Autonomous Region (NJYT23109).
† Corresponding author.E-mail addresses: zsylt0416@163.com

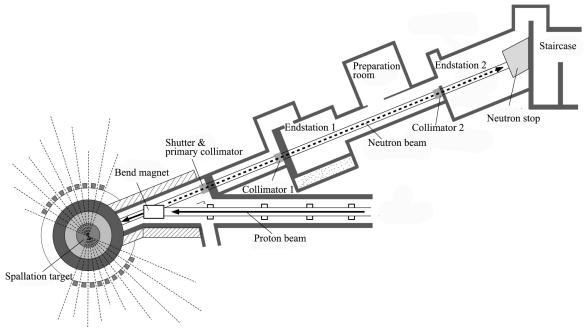

Fig. 1. (color online) Schematic view of the experimental setup of the CSNS Back-n [18].

data [22–25]. Therefore, much more neutron capture measurements of ^{165}Ho should be carried out for testing the accuracy of evaluated nuclear data and the available experimental data. This work present a new dataset of the ^{165}Ho(n, γ)^{166}Ho reaction in the neutron energy range from 1 eV to 1 MeV, which is measured by using the C_6D_6 detection system at the CSNS Back-n white neutron source. In the following sections, we outline the methods employed in the experiment and data analysis, discuss the reliability of results, and provide detailed information about the CERN ROOT code [26] relevant to this study.

II. METHODS

A. Measurement

In May 2022, measurement of the ^{165}Ho(n, γ)^{166}Ho reaction was performed at the CSNS Back-n experimental area (#ES2), where is located at flight path length of about 76 meters. The neutron beam was delivered at ES2 with about 6.92×10^5cm^{-2}s^{-1} neutrons per nominal pulse of 1.6×10^{13} protons in the energy range of 0.3 eV to 200 MeV of beam spots in ϕ30 mm. The neutron energy spectrum was determined using two different detectors, one being a Li-Si detector and the other being a calibrated fission chamber, which were based on the reactions of ^{6}Li(n, t) and ^{235}U(n, f), respectively [27, 28]. The neutron flux in the experiment was monitored by a silicon flux monitor (SiMon), consisting of a thin ^{6}LiF conversion layer and eight silicon detectors, approximately 20 meters upstream from the sample location. The γ-rays from the ^{165}Ho capture reaction were detected by a set of four C_6D_6 scintillators. The detectors were positioned approximately 17 cm from the target at an angle of 125 degrees relative to the neutron beam, as shown in figure 2. The characteristics of the samples used in this experiment, provided by the China Institute of Atomic Energy, are detailed in Table 1. A natural metallic holmium sample was employed to determine the neutron capture cross section of ^{165}Ho. A gold sample of the same dimensions as the holmium sample was utilized for measuring the neutron flux and normalizing the neutron capture data. Background measurements due to scattered neutrons and in-beam γ-rays were conducted using a lead sample. Additionally, an empty sample run was performed to evaluate the sample-independent background. Detector signals were recorded by the CSNS Back-n general-purpose Data Acquisition System [29], which operates at a sampling rate of 1 GS/s with 12-bit full-waveform digitizers. Data acquisition was triggered by the pickup signal from the proton beam. Dead time corrections were disregarded due to the lower event statistics observed in the present experiment. Total beam measurement time was 100 hours, and the CERN ROOT code was utilized for offline analysis.

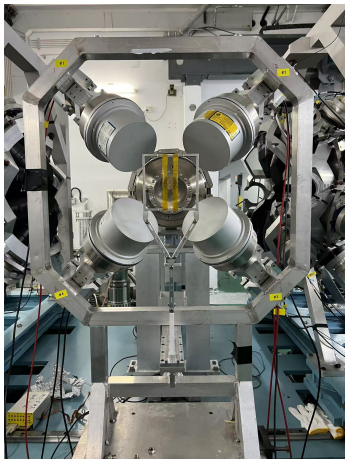

Fig. 2. (color online) The setup of the four C_6D_6 detectors in the measurement. The detectors were positioned approximately 17 cm from the target at an angle of 125 degrees relative to the neutron beam.

TABLE 1. Characteristic parameters of samples

Sample	Thickness (mm)	Diameter (mm)	Mass (mg)	Area desity ($atom \cdot b^{-1}$)
^{165}Ho	0.20	30	1243.32	6.42×10^{-4}
^{197}Au	0.10	30	1357.17	5.87×10^{-4}
^{nat}Pb	0.53	30	4249.75	1.75×10^{-3}
Empty holder				

B. Data analysis

The ^{nat}Pb sample data are parameterized as eq.(1) to evaluate the in-beam γ-rays and scattered-neutron background contributions for this experiment. The ^{165}Ho sample with the ^{181}Ta and ^{59}Co neutron filters are also performed and used to determine the normalization factors f_n and f_γ for B_n and B_γ components by matching the dips of the filtered spectra. The influence of the filters on in-beam γ-rays and neutrons is assessed carefully by analyzing the neutron flux and the energy distribution of the in-beam γ-rays [30]. Energy spectra of neutrons and γ-rays produced at spallation target are sampled randomly for the incident particle energy spectra of the GEANT4 Monte Carlo code [31], allowing for simulations both with and without filters. The counts of scattered neutrons and γ-rays are recorded at the detector position. The

reduced attenuation factors for neutrons and γ-rays are found to be 0.92 and 0.68, respectively, which are applied as corrections to f_n and f_γ. Much more information of evaluation method used in this work can be found in Ref. [12].

$$B(E_n) = f_\gamma B_\gamma(E_n) + f_n B_n(E_n) \quad (1)$$

where the B_γ and B_n denote the background contribution of the in-beam γ-rays and scattered neutrons, respectively, and can be formulated as eqs. (2-3).

$$B_\gamma(E_n) = b \times e^{-c/\sqrt{E_n}} + d \times e^{-e\times\sqrt{E_n}} + f \quad (2)$$

$$B_n(E_n) = \frac{a}{\sqrt{E_n}} \quad (3)$$

The experimental neutron capture yield as a function of neutron energy can be calculated as eq.(4)

$$Y_{exp}(E_n) = \frac{1}{f_n}\frac{S(E_n) - B(E_n)}{\epsilon_c \times \Phi(E_n)} \quad (4)$$

where E_n is the incident neutron energy converted from the neutron time-of-flight (TOF) spectra using the relativistic relation. $S(E_n)$ is the count spectrum of the ^{165}Ho sample, $B(E_n)$ is the evaluated background, $\Phi(E_n)$ is the neutron flux spectrum. The normalization factor f_n, determined by self-normalizing the measured capture yield of 4.9 eV resonance of ^{197}Au, accounts for the absolute incident neutron flux. The ϵ_c is the detection efficiency of a capture event. The total energy detection principle was used, combining the above-mentioned C_6D_6 detection system with the pulse height weighting technique (PHWT) [32, 33], to achieve the proportionality between the ϵ_c and the total γ-ray energy (E_c)) released in the capture event. Hence, $\epsilon_c = kE_c = k(S_n + E_{cm})$, where S_n is the neutron separation energy (i.e. 6.24 MeV) of the compound nucleus, and E_{cm} is the center-of-mass energy of the incident neutron. In the analysis of the ^{165}Ho(n,γ)^{166}Ho measurement, the threshold established are E_{dep}^{min}=250 keV and E_{dep}^{max}=7 MeV, corresponding to the Compton edges for γ-ray energies of 124 keV and 6.75 MeV, respectively. The weighted function (WF) as a 5^{th} polynomial function are fitted with Geant4 Monte Carlo code, simulating the C_6D_6 detector response for 27 different monoenergetic γ-rays from 0.1 MeV to 10 MeV. This WF was then applied to all the $S(E_n)$ and $B(E_n)$ spectra for following data analysis.

The resonance shape analysis code SAMMY [34] was used to fit the measured neutron capture yield calculated by eq.(4). In the SAMMY code, the reaction cross section data is described by a multi-level Reich-Moore formalism, which only depends on the properties of the nuclear excitation. This code takes into account all the experimental conditions such as multiple interacting events, sample characteristics, self-shielding, the broadening of resonances due to thermal motion and experimental resolution of the CSNS Back-n facility [35]. In the fitting process, the initial resonance parameters were taken from the evaluated nuclear data library ENDF/B-VIII.0 [36] and iteratively refined until convergence. The resonance parameters, including resonance energy and capture kernels, were determined using SAMMY fits within the resonance region up to 100 eV, where individual neutron resonances were fitted with high precision. Based on these resonance parameters, the resonance cross sections for the ^{165}Ho(n, γ)^{166}Ho reaction were reconstructed. However, resonance structures could not be adequately resolved beyond approximately 100 eV due to the deterioration of experimental resolution and reduced event statistics as the neutron energy increased. Consequently, an averaged neutron capture cross section was directly derived from the measured neutron capture yield in unresolved resonance range using the formula (5), where N_s represent the sample's areal density. In this case, the measured capture yield was corrected for multiple scattering and self-shielding effects through Geant4 code that accounts for the sample composition, geometry, and both neutron scattering and capture cross sections. Subsequently, the ^{165}Ho neutron capture cross section was determined relative to the standard ^{197}Au sample [37] within the neutron energy range of 2 keV to 1 MeV.

$$\sigma_\gamma = \frac{Y_{exp}(E_n)}{N_s} \quad (5)$$

The uncertainties in the present experimental data arise from both statistical and systematic errors. The systematic errors were evaluated based on contributions from various sources. The energy dependent neutron flux shape contributes an uncertainty of 4.5% below 150 keV and 8.0% above this threshold. Additionally, the uncertainty related to the normalization accounts for approximately 1%, while the calculation of PHWT introduces a contribution of 3% to the overall uncertainties. Furthermore, the uncertainty from background subtraction using filters is about 8.6%, and an additional uncertainty of 0.01% due to the sample impurities was also considered. The sum of these components yields an overall systematic uncertainty of 10.2%(12.2%) for the capture cross section.

III. DATA RECORDS

For each neutron pulse, data from three different types of detectors are simultaneously recorded and stored. One type is a proton beam counter, monitored by the pick-up detector of the Proton Synchrotron accelerator. The second type is a neutron flux counter, composed of eight SiMon detectors. These two data types are utilized for cross-validation and normalization of various measurements. The third type of data includes the event information for radiative neutron capture, recorded by four C_6D_6 scintillator detectors. All the aforementioned data are acquired using a fully digital data acquisition (DAQ) system of the CSNS Back-n [29], with event-by-event connectivity on the basis of CERN ROOT code. For each neutron capture event, both of the deposited energy, represented as a pulse height spectrum in the C_6D_6 detector, and TOF information of the incident neutrons are recorded. Table 2 lists

a comprehensive summary of the event information for all samples utilized in the measurement. The data records are organized in Tree format according to the CERN ROOT version 5.34 and consist of two branch datasets: "NeuDataTree" and "SiDataTree". "NeuDataTree" recorded data from four C_6D_6 detectors, including nine leaves: GPSsec (triggering time in seconds), GPSnsec (triggering time in nanoseconds), T0id (trigger T0 identification number), BCid (detector identification number), Energy (neutron energy spectrum), Tof (time-of-flight spectrum), Ph (pulse height spectrum), PeakValue (pulse amplitude), and PeakPoint (pulse timing information). "SiDataTree", on the other hand, contained data from eight SiMon detectors, organized into six leaves: GPSsec (triggering time in seconds), GPSnsec (triggering time in nanoseconds), T0id (trigger T0 identification number), BCid(detector identification number), SiTof (time-of-flight spectrum), and SiPeakValue (pulse amplitude). This structured organization of data enables efficient storage and facilitates detailed analysis of time, energy, and spectral characteristics captured by the detectors.

TABLE 2. Summary of the event information for all samples.

Sample	Measurement time	Document Number	Number of Files
^{165}Ho	52h56m	15935,15955	1085
^{197}Au	5h16m	15927,15946	102
^{nat}Pb	9h41m	15931,15950	182
Empty holder	12h48m	15944,15956	190

All raw data described in this paper have been uploaded in the Science Data Bank. A direct link to the dataset is available at (https://doi.org/10.57760/sciencedb.21041).

IV. TECHNICAL VALIDATION

Figure 3 presents the SAMMY fits (red lines) compared to the measured capture yields (black circles) for the reaction ^{165}Ho(n, γ)^{166}Ho across neutron energy ranges below 100 eV. A good agreement is observed between measurement and SAMMY fits, both in terms of resonance energy and spectral shape. The resonance energies E_R, radiative width Γ_γ, neutron width Γ_n and capture kernels k ($k = g\Gamma_n\Gamma_\gamma/(\Gamma_n + \Gamma_\gamma)$, g is the statistical factor) obtained in this study are compared with the data from the ENDF/B-VIII.0 library [36], as detailed in the Table 3. The experimental capture resonance parameters exhibit significant agreement with the ENDF/B-VIII.0 evaluations in the energy range below 100 eV. However, disparities are observed in the energy range between 100 eV and 2 keV, which can be ascribed to the degradation of experimental resolution function encountered at the CSNS Back-n facility during this measurement.

Figure 4 presents the comparison of the ^{165}Ho(n,γ)^{166}Ho cross sections between the TALYS-1.9 [38] calculations and the results reconstructed from SAMMY resonance fits for neutron energies below 100 eV. The measured neutron capture cross sections, ranging from 2 keV to 1 MeV, are displayed together with the calculated results from TALYS-1.9 and the evaluated data derived from the ENDF/B-VIII.0 library [36] in Figure 5. These comparisons demonstrate that the cross sections determined in this work are accurately reproduced by both the TALYS-1.9 calculations and the evaluated data across the full neutron energy range investigated. These results indicate that the experimental apparatus and data analysis methodologies have performed reliably and effectively.

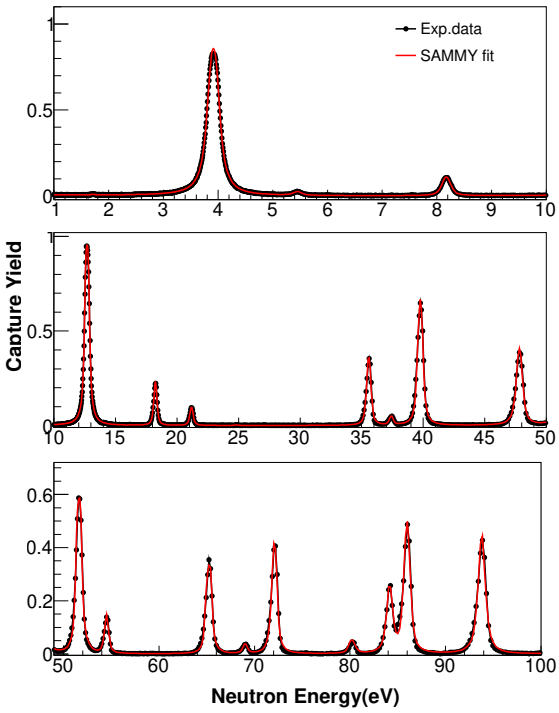

Fig. 3. (color online) SAMMY fits (red lines) to the measured capture yields (black circles) of ^{165}Ho(n, γ)^{166}Ho reaction.

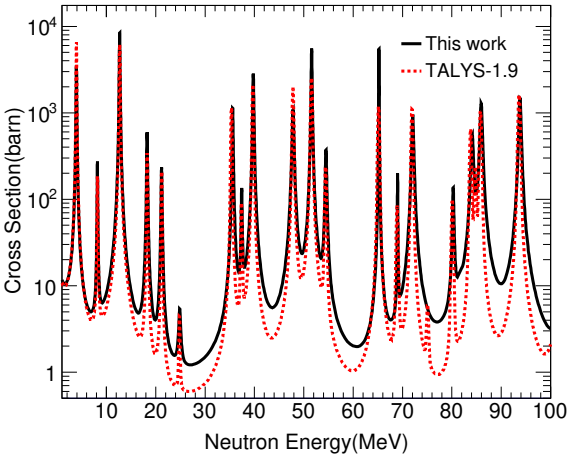

Fig. 4. (color online) Comparison of ^{165}Ho(n, γ)^{166}Ho cross sections, reconstructed from SAMMY resonance fits up to 100 eV neutron energy with the calculations from TALYS code version 1.9 [38].

TABLE 3. Resonance parameters up to 100 eV neutron energy for the ^{165}Ho (n, γ) cross sections.

J	This work				ENDF/B-VIII.0			
	E_R(eV)	$\Gamma_n(meV)$	$\Gamma_\gamma(meV)$	k	E_R(eV)	$\Gamma_n(meV)$	$\Gamma_\gamma(meV)$	k
4	3.91 ± 0.01	1.28 ± 0.01	129.10 ± 0.13	0.71 ± 0.01	3.91	2.13	85.70	1.17
3	8.17 ± 0.02	0.20 ± 0.01	98.66 ± 0.06	0.09 ± 0.01	8.17	0.19	90.30	0.08
4	12.68 ± 0.07	11.73 ± 0.15	122.82 ± 0.17	6.02 ± 0.04	12.69	10.31	84.00	5.17
3	18.24 ± 0.02	1.56 ± 0.18	159.76 ± 0.45	0.67 ± 0.06	18.25	0.95	78.10	0.41
4	21.16 ± 0.04	0.58 ± 0.02	167.16 ± 0.13	0.32 ± 0.01	21.19	0.52	68.00	0.29
3	28.38 ± 0.10	0.01 ± 0.01	16.50 ± 0.26	0.00 ± 0.00	24.79	0.02	84.00	0.01
3	35.58 ± 0.02	7.01 ± 0.08	184.08 ± 0.50	2.95 ± 0.03	35.33	8.69	73.60	3.40
4	37.41 ± 0.08	0.52 ± 0.02	162.36 ± 0.28	0.29 ± 0.01	37.36	0.50	83.00	0.28
4	39.76 ± 0.02	17.98 ± 0.02	193.14 ± 0.36	9.25 ± 0.01	39.67	16.80	88.00	7.94
3	47.82 ± 0.03	16.56 ± 0.16	329.52 ± 0.64	6.90 ± 0.06	47.80	28.23	92.00	9.45
3	51.57 ± 0.02	129.27 ± 0.12	95.13 ± 0.13	23.98± 0.03	51.55	56.57	85.00	14.86
4	54.50 ± 0.04	3.55 ± 0.53	241.76 ± 0.94	1.97 ± 0.19	54.42	2.40	84.00	1.31
4	65.23 ± 0.03	17.11 ± 0.15	360.22 ± 0.65	9.19 ± 0.07	65.15	18.67	77.00	8.45
4	69.01 ± 0.12	1.14 ± 0.06	269.18 ± 0.37	0.64 ± 0.03	68.91	1.10	89.00	0.61
4	72.12 ± 0.03	20.31 ± 0.03	218.50 ± 0.67	10.45± 0.02	71.93	20.44	74.00	9.01
3	-	-	-	-	75.08	0.09	84.00	0.04
4	80.30 ± 0.04	3.69 ± 0.08	1.80 ± 0.24	0.68 ± 0.03	80.10	1.55	82.00	0.85
4	-	-	-	-	83.80	13.51	67.00	6.32
3	84.15 ± 0.07	20.08 ± 0.05	397.93 ± 0.20	10.75± 0.02	84.73	5.60	84.00	2.30
3	85.96 ± 0.32	46.34 ± 0.68	293.48 ± 0.89	24.08± 0.17	85.80	37.37	84.00	11.32
4	93.80 ± 0.03	45.31 ± 0.33	515.19 ± 0.72	23.43± 0.13	93.63	73.78	79.00	21.46

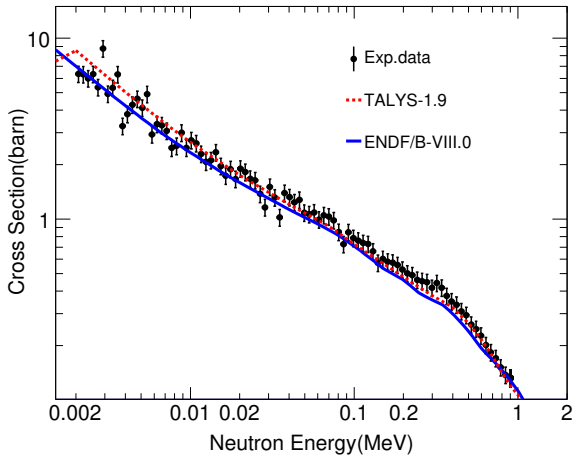

Fig. 5. (color online) Comparisons of the measured neutron capture cross section on ^{165}Ho of this work with the TALYS-1.9 calculations [38] and ENDF/B-VIII.0 evaluated data [36] in the 2 keV to 1 MeV.

V. USAGE NOTES

The dataset publication presents newly measured cross sections for the ^{165}Ho(n, γ)^{166}Ho reaction obtained with the CSNS Back-n facility. Our objective is to comprehensively document the data analysis procedures in a dedicated publication, thereby providing access to the neutron capture data for both the nuclear physics community and researchers in related disciplines for future studies. This dataset has numerous applications in nuclear physics, particularly in the following areas:

(1) The spectroscopic information of heavy nuclei is challenging to obtain experimentally due to the rapid increase in nuclear level density (NLD) with rising excitation energies. To address this, statistical models provide a framework for understanding the internal structure of these nuclei at higher energies, relying on key parameters such as the NLD and the γ-ray strength function (γSF). These parameters are essential for a wide array of calculations in nuclear reactions, particularly in determining neutron capture reaction cross sections. The accuracy of these calculations is vital for evaluating the reliability of nuclear models. In this context, the case of ^{166}Ho, an odd-odd deformed nucleus, plays a significant role. The ^{165}Ho(n, γ)^{166}Ho neutron capture reaction serves as a crucial tool for validating theoretical descriptions of the NLD and γSF. By examining this reaction, researchers can test and refine the predictive power of nuclear models, thereby enhancing our understanding of the underlying nuclear structure and reaction dynamics.

(2) The nucleosynthesis of elements heavier than iron is considered one of the ”11 Biggest Unsolved Mysteries in Physics” that require urgent attention this century. Nuclear astrophysicists generally agree that the slow neutron capture process (s-process) and the rapid neutron capture process (r-process) are the primary mechanisms responsible for the production of these heavier elements. Holmium, an important rare earth element, is primarily produced through explosive r-

process nucleosynthesis, with approximately 9% of its abundance synthesised in the main s-process during the evolution of intermediate-mass stars. The isotope ^{166}Ho is a significant branching nucleus, characterised by a ground state half-life of 26.9 hours and an isomeric state (7^-) half-life of 1200 years, primarily formed by the capture of a neutron by ^{165}Ho. Consequently, the ^{165}Ho(n, γ)^{166}Ho reaction not only depletes the abundance of ^{165}Ho but also influences the abundance of ^{166}Ho and subsequent s-process nucleosynthesis products. Therefore, this reaction cross section is critically important for the study of nucleosynthesis in nuclear astrophysics.

(3) Holmium (Ho) has extensive applications in nuclear medicine, particularly the β^- and γ-emitting isotope ^{166}Ho[$T_{1/2}$=26.9 h, E_β = 1.77 MeV (48%) and 1.85 (51%) MeV, E_γ = 81keV (6.7%)], which has been developed for radionuclide therapy and single photon emission computed tomography (SPECT) imaging due to its favourable decay properties. The isotope ^{165}Ho is the only naturally stable isotope of holmium (^{nat}Ho) and is used to produce ^{166}Ho through the (n, γ) reaction. Accurate data on the neutron capture cross section and resonance integral for the ^{165}Ho(n, γ)^{166}Ho reaction are essential for evaluating neutron irradiation time, activity, and yield of ^{166}Ho produced in nuclear reactors.

VI. CODE AVAILABILITY

The publication of the dataset is accompanied by a software package based on CERN ROOT version 5.34/34 [26], which includes examples for reading the data, generating pulse height spectra of neutrons, performing background subtraction, analyzing neutron resonances, and deriving neutron capture cross sections.

In the dataset, the neutron energy range from 0.2 eV to 2 MeV was logarithmically divided into 3500 bins. The bin intervals and quantities can be reallocated according to the user's range of interest. Two classes, C_6D_6 Data and LiSi Data, are defined to read the corresponding data from the ROOT file. The TChain function is used to read all ROOT files under the same experimental conditions. For the C_6D_6 data, the neutron energy thresholds were set to E_{dep}^{min}=250 keV and E_{dep}^{max}=7 MeV, with the following detector parameters:

$C_6D_6 : 1 \quad C_6D_6Data_1.BCid = 1, \quad Min : bin = 2822, \quad Max : bin = 78865;$

$C_6D_6 : 2 \quad C_6D_6Data_1.BCid = 2, \quad Min : bin = 2822, \quad Max : bin = 78865;$

$C_6D_6 : 3 \quad C_6D_6Data_1.BCid = 3, \quad Min : bin = 2807, \quad Max : bin = 78342;$

$C_6D_6 : 4 \quad C_6D_6Data_1.BCid = 4, \quad Min : bin = 2890, \quad Max : bin = 80629;$

For the LiSi data, the signals from eight LiSi detectors were divided into two paths for storage, with the parameters being as follows:

$LiSi : 1 \quad LiSiData_1.BCid = 5$

$LiSi : 1 \quad LiSiData_1.BCid = 6$

During the in-beam experiment, there was an issue with the second signal from the LiSi detector ($LiSiData_1.BCid = 6$), so the first signal($LiSiData_1.BCid = 5$) was chosen for data processing. The reaction between neutrons and ^{6}Li primarily generates helium nuclei (α) and tritium nuclei (T), resulting in a bimodal structure in the energy spectrum. Due to the high energy of the T peak (2.73 MeV), saturation may occur during the experiment, leading to poor statistical performance. Therefore, the α peak is selected as the effective neutron counting of the LiSi detector to determine the neutron flux. More detailed information about the data analysis code can be accessed as a notebook on the Science Data Bank, where the complete dataset for this work has been uploaded. A direct link to the dataset is available at:(https://doi.org/10.57760/sciencedb.21041).

ACKNOWLEDGEMENTS

Authors thanks to the efforts of the CSNS Back-n operators for the skilled operation of the facility. We would like to express thanks to Hong-Wei Wang, Xi-Chao Ruan and Jing-Yu Tang for their helpful comments to the measurement. And also thank to Qi-Wen Fan for preparing the samples.

AUTHOR CONTRIBUTIONS STATEMENT

Su-Ya-La-Tu Zhang Conceptualization, Methodology, Writing-review & editing. Yong-Shun Huang Investigation, Data curation, Writing-original draft. Wei Jiang, Jie Ren and Rui-Rui Fan Measurement, Methodology. De-Xin Wang Formal analysis. Guo-Li and Dan-Dan Niu Measurement. Chun-Lei Zhang Editing & English grammer correction. Mei-Rong Huang Writing- review & editing. All authors reviewed the manuscript.

COMPETING INTERESTS

The authors declare that they have no known competing financial interests or personal relationships that could have appeared to influence the work reported in this paper.

VII. REFERENCES

[1] Z.G. Ge, Y.J. Chen, Status and prospects of nuclear data development in China, Chin. Sci. Bull. 60 (32), 3087(2015). https://doi.org/10.1360/N972015-00694

[2] The n_TOF Collaboration, Nuclear data activities at the n_TOF facility at CERN. Eur. Phys. J. Plus 131, 371(2016). https://doi.org/10.1140/epjp/i2016-16371-4

[3] X.C. Ruan, Progress and prospect of neutron nuclear data measurement. SCIENTIA SINICA Physica, Mechanica & Astronomica 50(5), 052002(2020). https://doi.org/10.1360/SSPMA-2019-0231

[4] Z.Q. Chen, Recent progress in nuclear data measurement for ADS at IMP, Nucl. Sci. and Tech. 28, 184(2017). https://doi.org/10.1007/s41365-017-0335-3

[5] S. Zhang, Y.B. Nie, J. Ren, *et al.*, Benchmarking of JEFF-3.2, FENDL-3.0 and TENDL-2014 evaluated data for tungsten with 14.8 MeV neutrons, Nucl. Sci. and Tech. 28, 27(2017). https://doi.org/10.1007/s41365-017-0192-0

[6] C. Guerrero, J. Lerendegui-Marco1, M. Paul, *et al.*, Neutron capture on the s-process branching point ^{171}Tm via time-of-flight and activation. Phys. Rev. Lett. 125(142701), 1(2020) https://doi.org/10.1103/PhysRevLett.125.142701

[7] I. Knapova, A. Couture, C. Fry, *et al.*, Photon strength functions, level densities, and isomeric ratio in ^{168}Er from the radiative neutron capture measured at the DANCE facility, Phys. Rev. C 107(4), 044313(2023). https://doi.org/10.1103/PhysRevC.107.044313

[8] K. Wisshak, F. Voss, F. KÃ¤ppeler, *et al.*, Stellar neutron capture cross sections of the Lu isotopes, Phys. Rev. C 73(1), 015807(2006). https://doi.org/10.1103/PhysRevC.73.015807

[9] C.J. Prokop, A. Couture, S. Jones, *et al.*, Measurement of the ^{65}Cu(n, γ) cross section using the Detector for Advanced Neutron Capture Experiments at LANL, Phys. Rev. C 99(5),055809(2019). https://doi.org/10.1103/PhysRevC.99.055809

[10] J. Tang, R. Liu, G. Zhang, *et al.*, Initial years' neutron-induced cross-section measurements at the CSNS Back-n white neutron source, Chin. Phys. C 45(6), 062001(2021). https://doi.org/10.1088/1674-1137/abf138

[11] J. Ren, X. Ruan, W. Jiang, *et al.*, Neutron capture cross section of ^{169}Tm measured at the CSNS Back-n facility in the energy region from 30 to 300 keV, Chin. Phys. C 46(4), 044002(2022). https://doi.org/10.1088/1674-1137/ac4589

[12] S. Zhang, G. Li, W. Jiang, *et al.*, Measurement of the ^{159}Tb(n,γ) cross section at the CSNS Back-n facility. Phys. Rev. C 107, 045809(2023). https://doi.org/10.1103/PhysRevC.107.045809

[13] D. X. Wang, S. Zhang, W. Jiang, *et al.*, Resonance analysis of ^{159}Tb(n,γ) reaction based on the CSNS Back-n experiment. Nucl. Sci. Tech. 36, 43 (2025). https://doi.org/10.1007/s41365-024-01617-9

[14] L. Xie, P. Cao, T. Yu, *et al.*, Real-time digital trigger system for GTAF-II at CSNS Back-n white neutron source, J. Inst.16(10), P10029(2021). https://doi.org/10.1088/1748-0221/16/10/P10029

[15] Y. Yang, Z. Wen, Z. Han, *et al.*, A multi-cell fission chamber for fission cross-section measurements at the Back-n white neutron beam of CSNS, Nucl. Instrum. Methods Phys. Res. A 940, 486(2019). https://doi.org/10.1016/j.nima.2019.06.014

[16] J.M. Xue, S. Feng, Y.H. Chen, *et al.*, Measurement of the neutron-induced total cross sections of ^{nat}Pb from 0.3 eV to 20 MeV on the Back-n at CSNS, Nucl. Sci. and Tech. 35, 18(2024). https://doi.org/10.1007/s41365-024-01370-z

[17] W. Jiang, H.Y. Bai, H.Y. Jiang,*et al.*, Application of a silicon detector array in (n, lcp) reaction cross-section measurements at the CSNS Back-n white neutron source, Nucl. Instr. Methods A 973, 164126 (2020). https://doi.org/10.1016/j.nima.2020.164126

[18] J.Y. Tang, Q. An, J.B. Bai, *et al.*, Back-n white neutron source at CSNS and its applications, Nucl. Sci. and Tech. 32, 1(2021). https://doi.org/10.1007/s41365-021-00846-6

[19] J.B. Czirr, M.L. Stelts, Measurement of the neutron capture cross section of holmium-165 and gold-197, Nucl. Sci. and Eng. 52(3), 299(1973). https://doi.org/10.13182/NSE73-A19477

[20] R.L. Macklin, The ^{165}Ho (n,γ) Standard Cross Section from 3 to 450 keV, Nucl. Sci. and Eng. 59(3), 231(1976). https://doi.org/10.13182/NSE76-A26821

[21] A.D. Carlson, V.G. Pronyaev, D.L. Smith, *et al.*, International evaluation of neutron cross section standards, Nucl. Data Sheets 110(12), 3215(2009). https://doi.org/10.1016/j.nds.2009.11.001

[22] F. Pogliano, A.C. Larsen, S. Goriely, *et al.*, Experimentally constrained ^{165,166}Ho(n,γ) rates and implications for the s-process, Phys. Rev. C 107, 064614(2023). https://doi.org/10.1103/PhysRevC.107.064614

[23] W.P. Poenitz. Fast neutron capture and activation cross sections, Natl. Bur. Stand.(US), Spec. Publ.(United States) 425, 1975. https://www.osti.gov/biblio/7364993

[24] J.H. Gibbons, R.L. Macklin, P.D. Miller, *et al.*, Average radiative capture cross sections for 7-to 170-keV neutrons, Phys. Rev. 122(1), 182(1961). https://doi.org/10.1103/PhysRev.122.182

[25] J. Voignier, S. Joly, G. Grenier, Capture cross sections and gamma-ray spectra from the interaction of 0.5-to 3.0-MeV neutrons with nuclei in the mass range A= 45 to 238, Nucl. Sci. and Eng. 112(1), 87(1992). https://doi.org/10.13182/NSE91-92N

[26] R. Brun, F. Rademakers, ROOT-An object oriented data analysis framework, Nucl. Instr. Methods A 389, 81(1997). https://doi.org/10.1016/S0168-9002(97)00048-X

[27] Q. Li, G. Luan, J. Bao, *et al.*, The ^{6}LiF-silicon detector array developed for real-time neutron monitoring at white neutron beam at CSNS, Nucl. Instr. Methods A 946, 162497(2019). https://doi.org/10.1016/j.nima.2019.162497

[28] Y. Chen, G. Luan, J. Bao, *et al.*, Neutron energy spectrum measurement of the Back-n white neutron source at CSNS, Eur. Phys. J. A 55, 115 (2019). https://doi.org/10.1140/epja/i2019-12808-1

[29] Q. Wang, P. Cao, X. Qi, *et al.*, General-purpose readout electronics for white neutron source at China Spallation Neutron Source, Rev. Sci. Instrum. 89, 013511 (2018). https://doi.org/10.1063/1.5006346

[30] J. Ren, X. Ruan, W. Jiang, *et al.*, Background study for (n, γ) cross section measurements with C_6D_6 detectors at CSNS Back-n, Nucl. Instrum. Methods Phys. Res. A 985, 164703 (2021). https://doi.org/10.1016/j.nima.2020.164703

[31] S. Agostinelli, J. Allison, K. Amako, *et al.*, GEANT4-a simulation toolkit, Nucl. Instrum. Methods Phys. Res. A 506, 250 (2003). https://doi.org/10.1016/S0168-9002(03)01368-8

[32] U. Abbondanno, G. Aerts, H. Alvarez, *et al.*, New experimental validation of the pulse height weighting technique for capture cross-section measurements, Nucl. Instrum. Methods Phys. Res. A 521, 454 (2004). https://doi.org/10.1016/j.nima.2003.09.066

[33] G. L. Yang, Z. D. An, W. Jiang, et al. Measurement of Br(n,γ) cross sections up to stellar s-process temperatures at the CSNS Back-n. Nucl. Sci. and Tech. 34, 180 (2023). https://doi.org/10.1007/s41365-023-01337-6

[34] N.M. Larson, Updated user's guide for Sammy: Multilevel R-matrix fits to neutron data using Bayes' equations[R]. Oak

Ridge National Lab.(ORNL), Oak Ridge, TN (United States), 2008. https://doi.org/10.2172/941054

[35] B. Jiang, J. Han, W. Jiang, *et al.*, Monte-Carlo calculations of the energy resolution function with Geant4 for analyzing the neutron capture cross section of ^{232}Th measured at CSNS Back-n, Nucl. Instrum. Methods Phys. Res. A 1013, 165677 (2021). https://doi.org/10.1016/j.nima.2021.165677

[36] M.B. Chadwick, M. Herman, P. Oblozinsky, *et al.*, ENDF/B-VII.1 nuclear data for science and technology: cross sections, covariances, fission product yields and decay data, Nucl. Data Sheets 112(12), 2887(2011). https://doi.org/10.1016/j.nds.2011.11.002

[37] A.D. Carlson, V.G. Pronyaev, R. Capote, *et al.*, Evaluation of the neutron data standards, Nucl. Data Sheets, 148, 143(2018). https://doi.org/10.1016/j.nds.2018.02.002

[38] A.J. Koning, D. Rochman, J.C. Sublet, *et al.*. TENDL: complete nuclear data library for innovative nuclear science and technology[J]. Nucl. Data Sheets 155, 1(2019). https://doi.org/10.1016/j.nds.2019.01.002